Theoretical Analysis of Hydrophobic Matching and Membrane-Mediated Interactions in Lipid Bilayers Containing Gramicidin

Thad A. Harroun, William T. Heller, Thomas M. Weiss, Lin Yang, and Huey W. Huang*

Physics Department, Rice University, Houston, Texas 77251, USA

ABSTRACT   We present a quantitative analysis of the effects of hydrophobic matching and membrane-mediated protein-protein interactions exhibited by gramicidin embedded in dimyristoylphosphatidylcholine (DMPC) and dilauroylphosphatidyl-choline (DLPC) bilayers (Harroun et al., 1999. *Biophys. J.* 76:937–945). Incorporating gramicidin, at 1:10 peptide/lipid molar ratio, decreases the phosphate-to-phosphate (PtP) peak separation in the DMPC bilayer from 35.3 Å without gramicidin to 32.7 Å. In contrast, the same molar ratio of gramicidin in DLPC increases the PtP from 30.8 Å to 32.1 Å. Concurrently, x-ray in-plane scattering showed that the most probable nearest-neighbor separation between gramicidin channels was 26.8 Å in DLPC, but reduced to 23.3 Å in DMPC. In this paper we review the idea of hydrophobic matching in which the lipid bilayer deforms to match the hydrophobic surface of the embedded proteins. We use a simple elasticity theory, including thickness compression, tension, and splay terms to describe the membrane deformation. The energy of membrane deformation is compared with the energy cost of hydrophobic mismatch. We discuss the boundary conditions between a gramicidin channel and the lipid bilayer. We used a numerical method to solve the problem of membrane deformation profile in the presence of a high density of gramicidin channels and ran computer simulations of 81 gramicidin channels to find the equilibrium distributions of the channels in the plane of the bilayer. The simulations contain four parameters: bilayer thickness compressibility $1/B$, bilayer bending rigidity K_c, the channel-bilayer mismatch D_o, and the slope of the interface at the lipid-protein boundary s. B, K_c, and D_o were experimentally measured; the only free parameter is s. The value of s is determined by the requirement that the theory produces the experimental values of bilayer thinning by gramicidin and the shift in the peak position of the in-plane scattering due to membrane-mediated channel-channel interactions. We show that both hydrophobic matching and membrane-mediated interactions can be understood by the simple elasticity theory.

INTRODUCTION

In a previous paper (Harroun et al., 1999; henceforth denoted as paper I) the ideas of hydrophobic matching between a lipid bilayer and an embedded protein, and the resulting protein-protein interactions were probed directly in dilauroylphosphatidylcholine (DLPC) and dimyristoylphosphatidylcholine (DMPC) bilayers containing gramicidin channels. We found that the average phosphate-to-phosphate distance (PtP) of DLPC bilayer increased from 30.8 Å in its pure form to 32.1 Å with gramicidin incorporated at a concentration of 1:10 peptide/lipid molar ratio. Correspondingly, the PtP of DMPC bilayer decreased from 35.3 Å to 32.7 Å. Two bilayers of different thicknesses in the hydrocarbon region converge toward a common thickness corresponding to that of the gramicidin channel. If membrane deformation induces protein-protein attractions, one expects the effect to be stronger in DMPC, because on average DMPC thinned twice as much as DLPC expanded. Indeed we found that the most probable nearest-neighbor distance was 26.8 Å in DLPC, but the distance was reduced to 23.3 Å in DMPC, apparently because of membrane-mediated attractions. These results were obtained from x-

ray lamellar diffraction and in-plane scattering. They constitute clear experimental evidence of hydrophobic matching and membrane-mediated protein-protein attractive interactions. In this second paper, we present theoretical analyses of these experimental results in terms of the elastic properties of lipid bilayers.

Because lipid bilayers are more deformable than globular proteins (paper I), one assumes that in the action of hydrophobic matching the bilayer deforms to match the protein, whereas the structure of the protein is unchanged. Generally speaking, there are two different theoretical approaches to membrane deformation. The first approach treats the membrane deformation with a continuum theory. The energetics of deformation are expressed as a function of the material properties of the membrane, such as bending rigidity and thickness compressibility. The second approach uses molecular models. The basic constants for the second approach vary with the model. Here we will confine ourselves to the first approach (see Mouritsen and Bloom, 1993, for reviews on molecular models).

The early theoretical studies addressing the effects of proteins on membranes considered two modes of membrane deformation. Essentially these theories adopted a Landau free energy (Landau and Lifshitz, 1969) expanded in an order parameter and its in-plane gradient (Marcelja, 1976; Schroeder, 1977; Owicki and McConnell, 1979; Pearson et al., 1984). The common order parameter in these theories is the variation of the hydrocarbon thickness, D, from its unperturbed value h_o or, equivalently, the variation of the

in-plane cross-sectional area of the lipid molecule. The equivalency is the result of constant hydrocarbon volume; in other words, hydrocarbons are deformable but incompressible. The two lowest-order terms in the expansion of Landau free energy f_L are $f_L = (h_oB/2)(D/h_o)^2 + (\gamma/4)(\boldsymbol{\nabla}D)^2 + \ldots$, where $\boldsymbol{\nabla} = (\partial/\partial x, \partial/\partial y)$ is the in-plane gradient and the expansion coefficients include the thickness compressibility $1/B \ (= -(1/h_o)(\partial D/\partial P)$, where P is the normal pressure) and the bilayer tension coefficient 2γ. It follows that the local deformation induced by hydrophobic matching falls off exponentially with a decay length $\zeta = (h_o\gamma/2B)^{1/2}$ (Owicki and McConnell, 1979). Typical experimental values of h_o, γ, and B give $\zeta \approx 3$ Å (Huang, 1986). Estimates by a molecular model also gave $\zeta \approx 3$–6 Å (Fattal and Ben-Shaul, 1993).

These tension theories cannot explain the membrane thickness effect on gramicidin channel lifetime. The experiment by Elliott et al. (1983) showed that the mean channel lifetime decreases from 286 s in bilayers of $h_o = 21.7$ Å to 0.7 s in bilayers of $h_o = 28.5$ Å. The forces created by tension are one order of magnitude too small to effect such changes in channel lifetime (Elliott et al., 1983; Huang, 1986). This problem was resolved by introducing a more complete membrane deformation free energy including compression, tension, as well as splay terms (Huang, 1986, 1995). The part pertaining to thickness deformation is given by f_D:

$$f_D = \frac{h_oB}{2}\left(\frac{D}{h_o}\right)^2 + \frac{\gamma}{4}(\boldsymbol{\nabla}D)^2 + \frac{h_oK_1}{8}(\boldsymbol{\nabla}^2D)^2 \qquad (1)$$

where $\boldsymbol{\nabla}^2 = \partial^2/\partial x^2 + \partial^2/\partial y^2$. The derivation of this free energy was based on the elasticity theory for liquid crystals (de Gennes, 1969), where the splay modulus K_1 was defined. The splay term is directly related to the bending energy of the bilayer, $h_oK_1 = K_c$; the latter is the bending rigidity of the bilayer (Helfrich, 1973). This connection is apparent if we express the complete free energy of membrane deformation in terms of the displacements of the upper and lower hydrophilic-hydrophobic interfaces, u_+ and u_- (Huang, 1986):

$$f = \frac{h_oB}{2}\left(\frac{u_+ - u_-}{h_o}\right)^2 + \frac{\gamma}{2}[(\boldsymbol{\nabla}u_+)^2 + (\boldsymbol{\nabla}u_-)^2]$$

$$+ \frac{K_c}{4}[(\boldsymbol{\nabla}^2u_+)^2 + (\boldsymbol{\nabla}^2u_-)^2] \qquad (2)$$

$$= \frac{h_oB}{2}\left(\frac{D}{h_o}\right)^2 + \frac{\gamma}{4}(\boldsymbol{\nabla}D)^2 + \frac{K_c}{8}(\boldsymbol{\nabla}^2D)^2$$

$$+ \gamma(\boldsymbol{\nabla}M)^2 + \frac{K_c}{2}(\boldsymbol{\nabla}^2M)^2$$

In the form expressed in the first line, the bilayer deformation free energy consists of a compression term and tension and bending energies of two monolayers. Note that the tension of each monolayer is γ, and the bending rigidity of

each monolayer $K_c/2$ is one-half of the bilayer value. In the second line of Eq. 2, the free energy is expressed in terms of the thickness variation $D = u_+ - u_-$ and the deviation of the midplane of the bilayer from its unperturbed, planar configuration on the x-y plane, $M = (u_+ + u_-)/2$. The spontaneous curvatures have been assumed to be zero for DLPC and DMPC monolayers (Seddon, 1989).

The D-mode, or the thickness deformation mode, and the M-mode, or the out-of-plane fluctuation mode, are decoupled in this free energy; therefore, these two modes of deformation are independent of each other. The elasticity coefficients were chosen so that the tension coefficient and the bending rigidity of the bilayer, as usually measured in the M-mode, are 2γ and K_c, respectively. Note that the coefficient of the curvature term is $K_c/2$ for the M-mode but is $K_c/8$ for the D-mode.

Based on the experimental values of B, γ, and K_c, it is easy to show that tension is important only for long-range ($\gg$10 nm) deformation, such as long-wavelength undulation fluctuations. But for local deformations, such as those caused by hydrophobic mismatch, the tension term contributes $<5\%$ of the total energy (Huang, 1986). Recently Goulian et al. (1998) demonstrated that the effect of externally applied membrane tension on the gramicidin channel lifetime is entirely through its membrane thinning effect (rather than its "pulling" effect on the gramicidin channel)—as a result, externally applied tension increases rather than decreases the channel lifetime. This is the clearest demonstration that the tension term in Eq. 1 plays an insignificant role in the energetics of locally induced deformations.

Another important consequence of the free energy (1) is that the characteristic length is now $\lambda = (h_oK_c/4B)^{1/4} \approx 13$ Å, instead of $\zeta = (h_o\gamma/2B)^{1/2} \approx 3$ Å. Furthermore, the thickness deformation profile often contains an inflection point due to an interplay between splay and compression. As a result, a local deformation often propagates over several λ's, and the membrane-mediated interactions may extend over 30–50 nm (Huang, 1986).

The majority of recent theoretical work has focused on refinements of the free energy (1), including protein-lipid boundary conditions (Dan et al., 1994), induced spontaneous curvature by protein inclusion (Dan et al., 1993; Aranda-Espinoza et al., 1996), and fluctuation-induced interactions (Goulian et al., 1993). A brief review of the recent work was given by Goulian (1996).

THICKNESS DEFORMATION AND BOUNDARY CONDITIONS

In Eq. 1 f_D represents the free energy of thickness deformation per unit area of the unperturbed bilayer. In the following we will neglect the tension term because of its insignificant contribution. Then the variational principle gives the Euler-Lagrange equation (Huang, 1986):

$$\boldsymbol{\nabla}^4D + \lambda^{-4}D = 0 \qquad (3)$$

The solution of Eq. 3, with appropriate boundary conditions at the lipid-protein contact, describes the effect of proteins on the membrane thickness profile. At this point one should examine the legitimacy of extending a continuum theory to the molecular scale. We believe that even on the molecular scale there is a well-defined, time-averaged molecular position for the interfaces. Therefore the thickness variation $D(x, y)$ can be defined. What is unknown is whether the elasticity coefficients measured on the macroscopic scale are still the same on the molecular scale (Boon and Yip, 1980). For this reason, we will have to allow some uncertainties in the values of B and K_c.

The solution of Eq. 3 contains four constants of integration that are to be determined by D and the slope of D at the protein boundaries (and at infinity). Let us first discuss the boundary value of D, designated as D_o. When we consider the energy cost of hydrophobic mismatch between membrane and protein, we should realize that the free energy of bilayer deformation is also rooted in the natural tendency of lipid molecules to maintain the hydrophobic matching condition in its bilayer formation. The stress of a deformed bilayer is primarily the result of hydrophobic interactions (Tanford, 1980; Israelachvili, 1992). In other words, the energy cost of hydrophobic mismatch and the membrane deformation energy are of the same nature. The idea of hydrophobic matching implicitly assumes that the former is larger than the latter. Is this always true? Gramicidin provides an example of this problem. An analytical expression for the deformation energy due to the insertion of a single gramicidin channel was derived by Huang (1986) according to the free energy equation (Eq. 1). Combining Eqs. IV.17 and IV.19 of Huang (1986) and using the experimental values for various constants, we arrived at a total deformation energy caused by one channel insertion $F_M = \iint f_D \, dx \, dy = 1.8 \times 10^{-14} \, D_o^2$ erg, where D_o is measured in Å. On the other hand, the energy of hydrophobic mismatch, i.e., the energy cost if matching does not occur, is estimated by the free energy change for transfer from organic solvent to water of nonpolar residues: 16.7 erg/cm^2 (Chothia, 1974). The external diameter of a gramicidin channel is 18 Å, so the area of mismatch is $18\pi D_o$ Å^2. This gives a mismatch energy $9.4 \times 10^{-14} \, D_o$ erg. Because the deformation energy is proportional to D_o^2, whereas the energy cost of mismatch is proportional to D_o, one expects hydrophobic matching to occur for small D_o, <5.3 Å according to the above estimate. For larger mismatches, some slippage or incomplete matching is expected to occur.

The slope of deformation, i.e., the derivative of D, at the protein boundary must be regarded as an effective parameter, not necessarily representing the real shape of molecular configurations, because we are extending a continuum theory to the molecular scale. There is no formula for determining the slope at the boundary. Helfrich and Jakobsson (1990) had proposed that the boundary condition of the slope adjusts itself to minimize the free energy of the bilayer deformation induced by the channel insertion. We believe this is incorrect for the following reason. Let s represent the

slope at the boundary. The equilibrium value of s is then determined by minimization of the total energy of the system with respect to s. However, the total energy consists of the membrane deformation energy $F_M(s)$ and the boundary energy $E_{bd}(s)$. The correct solution for s is that obtained from $F_{M'}(s) + E_{bd'}(s) = 0$ (where $'$ represents d/ds). As we noted above, the membrane energy and the boundary energy are of the same origin. Thus $F_{M'}(s)$ and $E_{bd'}(s)$ could be of the same order of magnitude. Helfrich and Jakobsson's proposition amounts to using $F_{M'}(s) = 0$, neglecting a potentially important term, $E_{bd'}(s)$. This point was also implied by Nielsen et al. (1998), who noted the disagreement of the assumption $F_{M'}(s) = 0$ with experimental results. In reality $E_{bd}(s)$ is unknown; the boundary condition of the slope can only be determined indirectly by experiment.

MEMBRANE THINNING AND PROTEIN CORRELATIONS BY SIMULATIONS

In principle, the free energy of Eq. 1 determines how the gramicidin channels are distributed in a lipid bilayer in thermal equilibrium. This is done by first calculating the thickness profile of the bilayer for a distribution of the channels. From the profile, the total energy of deformation F_M is calculated. The probability of this particular distribution of the channels is then proportional to the Boltzmann factor $\exp(-F_M/k_B T)$, where k_B is the Boltzmann constant and T is the absolute temperature. In principle, one can then calculate the average membrane thinning and the pair correlation function of the channels. However, to carry out these computations by analytical methods is difficult. For example, although the thickness deformation induced by a single channel can be solved analytically (Huang, 1986), the profile induced by more than two channels is analytically intractable.

The first theoretical analysis of membrane-mediated protein interactions (Pearson et al., 1984) obtained a two-particle interaction from a Landau theory and used a superposition of two-body interactions to approximate many-body interactions. A more recent analysis (Aranda-Espinoza et al., 1996) obtained a two-protein interaction potential based on Eq. 1 above, by arranging the proteins on a hexagonal lattice (the Wigner-Seitz cell). A solution of Eq. 3 was obtained by assuming radial symmetry, and the energy of membrane deformation as a function of the radius of the cell was used as the interaction potential between proteins in high densities. A radial distribution function was then obtained by the Percus-Yevick approximation (Hansen and McDonald, 1986). In both of these analyses, the many-body nature of the problem was not treated fully.

We believe that the interactions among many (>2) proteins in membrane cannot be reduced to two-body interactions. Therefore we have devised a numerical method for deriving the exact solution of Eq. 3 with an appropriate boundary condition at each gramicidin channel. Consider a square area of membrane containing a chosen density of

channels. Both the channel and the bilayer are symmetrical by reflection with respect to the bilayer's midplane ($M = 0$). We will use the variable $u = u_- = u_+ = D/2$ to describe one of the bilayer's deformed interfaces, $u(x, y)$ (Fig. 1 A). We approximate the channels as cylinders and assume the boundary condition at each channel as

$$u(r)|_{r=r_o} = u_o, \quad \frac{\partial}{\partial r} u(r)|_{r=r_o} = s \qquad (4)$$

where r is the radial coordinate from the center of a channel, r_o is the radius of the channel, $u_o = D_o/2$, and s is the radial gradient at the boundary. For simplicity the gradient has been assumed to be azimuthally symmetrical. For mathematical convenience, periodic boundary conditions are applied to the square area considered. Equation 3 was solved explicitly for $u(x, y)$ by using a finite difference method (details of the numerical method are described in the Appendix). As a test, the method was applied to the one-channel problem, which has an analytical solution (Huang,

FIGURE 1 (A) Schematic of a deformed bilayer matching the hydrophobic surface of a gramicidin channel (gray). The curves at $r \geq r_o$ represent the symmetrical profiles of two interfaces. We use $u(\mathbf{r})$, the displacement of the lower interface relative to its unperturbed position, to represent the deformation profile. At the channel radius r_o, $u = u_o$ as a boundary condition. (B) Numerical and analytical solutions of Eq. 3 for one channel with $\lambda = 10.62$ Å, $u_o = 1.5$ Å, $s = 0.0$. Note that the vertical scale is exaggerated relative to the scale of r for ease of comparison.

1986). The numerical solution is in complete agreement with the analytical solution (Fig. 1 B). This method makes no assumptions about the distribution of channels and is applicable to any number of channels. Examples of many-body solutions are shown in Fig. 2. Once the solution $u(x, y)$ is found, the energy of deformation per unit area (Eq. 1) can be integrated over the total membrane area to obtain the total deformation energy of the system F_M.

To find the equilibrium distribution of the channels in the membrane, we ran a computer simulation on our membrane patch. Eighty-one channels were distributed on a square lattice initially. After the energy F_M was calculated for that initial distribution, the channels were allowed to randomly diffuse to a new distribution. To do this, each channel was considered in turn to be moved by displacing its position by a random amount, uniformly chosen from the interval $[0, \Delta]$ along each of the coordinate directions x and y. A move that resulted in overlapping channels was not allowed and thus is equivalent to a simulation of hard disks. The maximum allowed displacement, Δ, is an adjustable parameter that controls the rate at which the ensemble of channels explores the phase space. With each move of a channel, the new deformation $u(x, y)$ and the corresponding total energy F_M were calculated. The new position for that channel was accepted if the change $\delta F_M = F_M(\text{new}) - F_M(\text{old}) < 0$. If $\delta F_M > 0$, the move was accepted with the Boltzmann probability: a number was randomly chosen in the interval $[0, 1]$. If that number was smaller than $\exp(-\delta F_M/k_B T)$, the new channel position was accepted; otherwise it was returned to its previous position. In the above process, if the step size Δ is too large, most moves would be rejected, and a new ensemble of channel positions would be generated very slowly. On the other hand, if Δ is too small, nearly all of the moves would be accepted, but then the phase space would be explored too slowly. Therefore, after each cycle, in which each channel had been considered once in turn for a move, the maximum step size Δ was adjusted so that on average, 50% of the moves were accepted. If the number of successful moves in a cycle of trials was too small, the step size was decreased by 4%; if too great, it was increased by 4%. This is a standard method for ensuring some efficiency in exploring the phase space (Allen and Tildesley, 1987). Furthermore, periodic boundary conditions were applied to the movement of the channels: if a channel stepped off one edge of the simulated area, another stepped onto the area from the opposite side.

It is well known that such a Metropolis Monte Carlo procedure evolves a system to its thermal equilibrium state (e.g., Allen and Tildesley, 1987). Fig. 3 shows the evolution of one simulation. We see that both F_M and the average of $u(x, y)$ over the entire membrane, denoted as $\langle u \rangle$, reach a steady state within 200 simulation cycles. We let the simulation continue for another 2000 cycles. The channel distribution generated by each of these final 2000 cycles represents one molecular configuration of the equilibrium state (Fig. 3). A histogram was made of the distance between every pair of channels after each cycle, and the total 2000
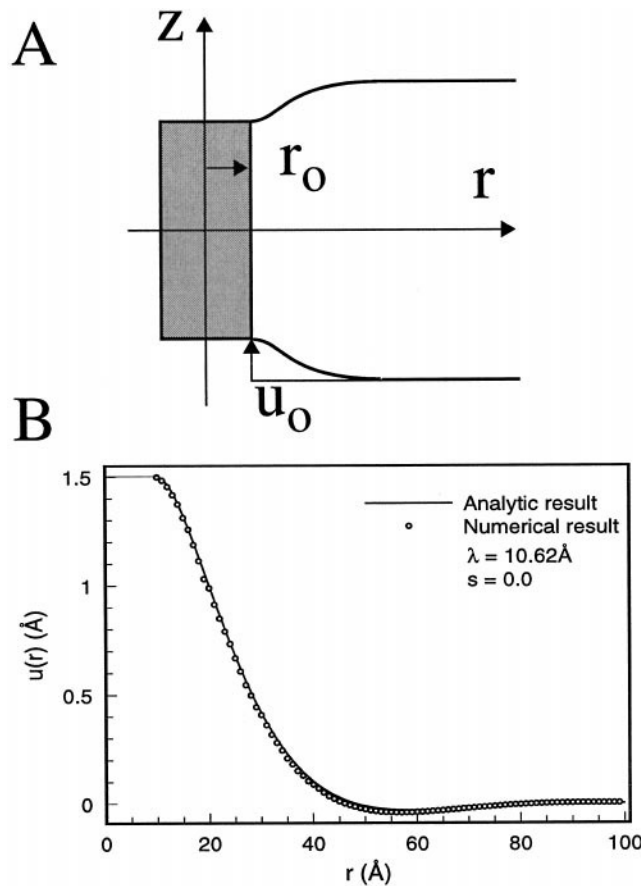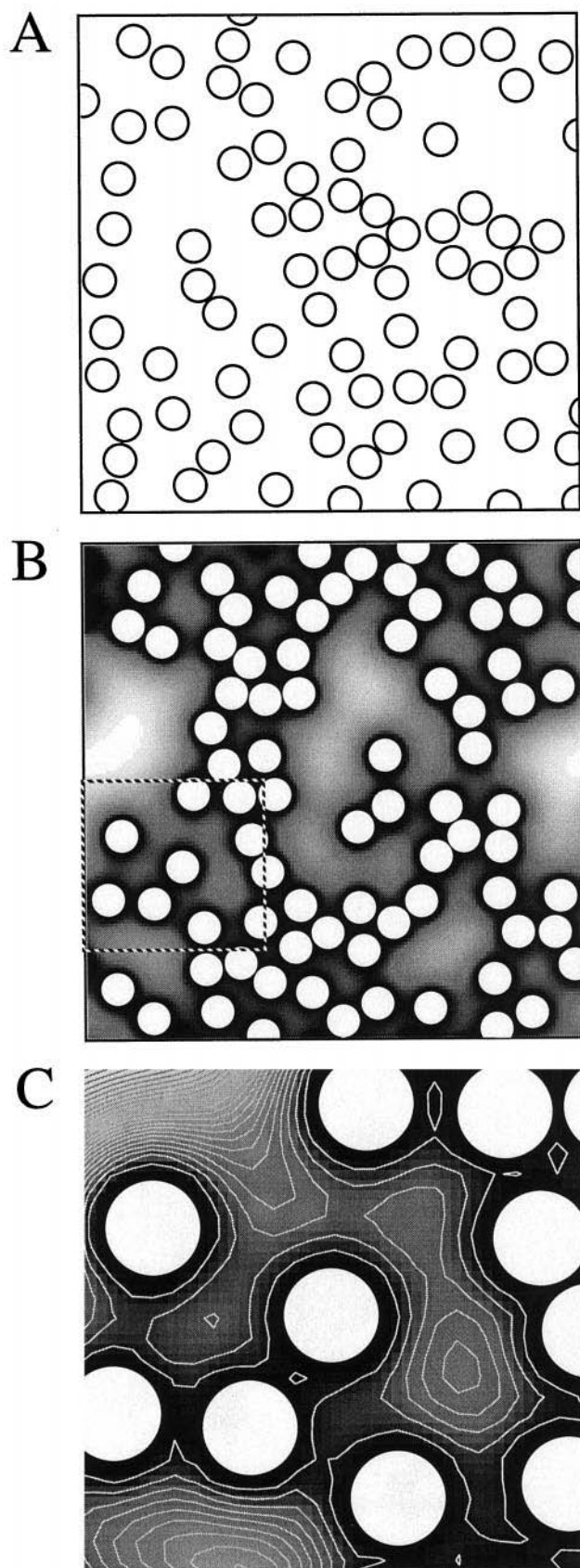
FIGURE 2 Examples of simulations. (*A*) A simulation of free hard disks. Circles represent gramicidin channels (or hard disks), 18 Å in diameter. There are no interactions between the channels other than the hard-core
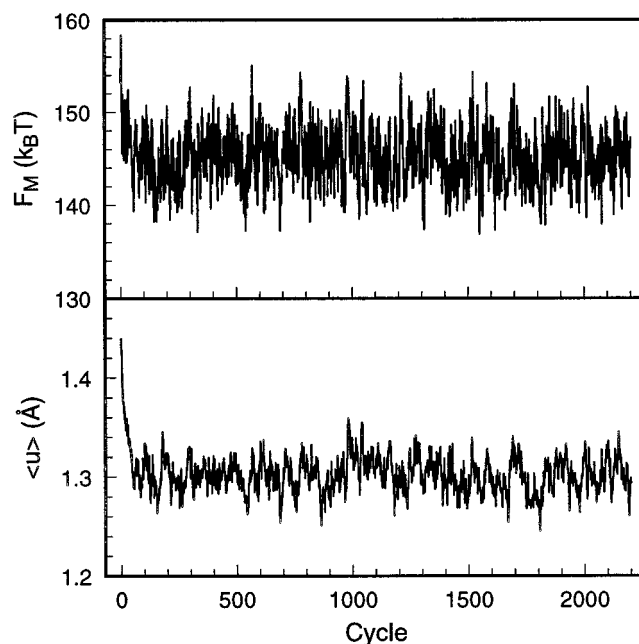

FIGURE 3 The energy of membrane deformation F_M and the average of (half) thinning $\langle u \rangle$ during the course of a simulation.

histograms were averaged together and normalized to generate the equilibrium pair-correlation function $n(r)$ (Eq. 2 in paper I). The pair correlation was then 2D Fourier transformed to obtain the structure factor $S(q)$ (He et al., 1993a, 1996). The average value of $u(x, y)$ and the energy F_M were each averaged over the final 2000 cycles to obtain the average membrane thinning $\langle u \rangle$ and the average deformation energy per channel $\langle F_M \rangle / N$.

The computation time for simulation scales linearly with the number of channels and quadratically with the number of finite difference mesh points used for the numerical calculation. For the majority of our simulations we used 81 gramicidin channels and a finite difference mesh spacing set to 20% of the channel diameter. To test whether the number of channels and the mesh size are reasonable, we ran two test simulations: one with a mesh size reduced by 50% and keeping the same number of channels, and another with the same mesh size but quadrupling the number of channels. The results of the test runs are essentially the same as those for our normal simulations. As a reference we also simulated channels with no mutual interactions other than hard-core repulsion (Fig. 2 *A*). The results were identical to published free hard disk simulations (Lado, 1968).

exclusion. (*B*) A simulation of channels (hard disks) in a membrane under the influence of Eq. 1. Membrane deformation induces interactions between channels in addition to the hard-core exclusion. The area outside of the circles is the membrane shown in a density plot. Darkness represents height depression. There are many more pairs of channels close to each other in *B* than in *A* because of membrane-mediated attractions in the former. (*C*) Blowup of a small patch of *B*, indicated by dotted lines. The contours indicate the membrane deformation $u(x, y)$.

COMPARISON WITH EXPERIMENT

Although the free energy (Eq. 1) contains two elasticity constants B and K_c (the γ term is neglected as stated above), the equation for $u(x, y)$ (Eq. 3) contains only one length scale λ. For a given λ, the actual length scale of deformation profile $u(x, y)$ is defined by the radius r_o. The area ratio occupied by the channels, called the areal density, is also an important characteristic of the problem. To determine r_o, we obtain the volume of gramicidin, 6192–6518 Å^3 per dimer, from the sizes of the crystalline unit cells (Wallace and Ravikumar, 1988; Lang, 1988). The length of the channel, 26 Å, was obtained from x-ray measurement of the divalent ion binding sites in the channel (Olah et al., 1991) or from the structure determined by NMR (Arseniev et al., 1985; Nicholson and Cross, 1989). Thus the cross-sectional area of the gramicidin channel is ~250 Å^2, which gives $r_o \approx 9$ Å. In an independent study by x-ray diffraction (Chen, Hung, and Huang, manuscript in preparation), we found that the in-plane cross-sectional area per lipid is ~62 Å^2 for each of DLPC and DMPC at a temperature ~10°C above its respective main transition temperature. Woolf and Roux (1996) also used 250 Å^2 for the cross section of the gramicidin channel and 62 Å^2 for the area of DMPC in their molecular dynamics studies. At a concentration of 10 lipids to 1 gramicidin, the areal density of the channels in both DLPC and DMPC bilayers is area(gD)/[10 area(DMPC) + area(gD)] = 0.29. All of our simulations used this areal density for the channels.

It is important to note that the peak position of the simulated $S(q)$ is directly proportional to the length scale set by the radius r_o and depends to some extent on the precise value of the areal density of channels. Therefore, instead of comparing the theoretical $S(q)$ directly with the experimental $S(q)$, we compare the simulations with the relative shift of its peak position between DMPC and DLPC. This relative shift should be most sensitive to the difference in the membrane-induced channel-channel interactions between DMPC and DLPC, but not sensitive to the precise values of r_o and the areal density of channels. Experimental $S(q)$ was obtained from the scattering intensity $I(q)$ divided by the form factor squared $|F(q)|^2$ (paper I). As noted in paper I, the form factor of gramicidin channel is a well-established quantity, because it is essentially determined by the peptide backbone alone. Thus we regard the peak position q_{max} of the experimental $S(q)$, as given in Fig. 4, to be as robust as the peak position of $I(q)$ (Fig. 6 of paper I). Relative to the peak position in the fluid DLPC, the correlation peak in the fluid DMPC is blue-shifted by 8%.

Our simulations contain only four parameters: the elasticity coefficients B and K_c, and the boundary conditions u_o and s:

1. B. Evans and Needham (Evans and Needham, 1987; Needham and Evans, 1988) measured the stretch coefficient K_a of DMPC by pipette aspiration to be 145 dyn/cm at 29°C. Assuming volume incompressibility for the hydrocarbon chains, one obtains the relation between the stretch
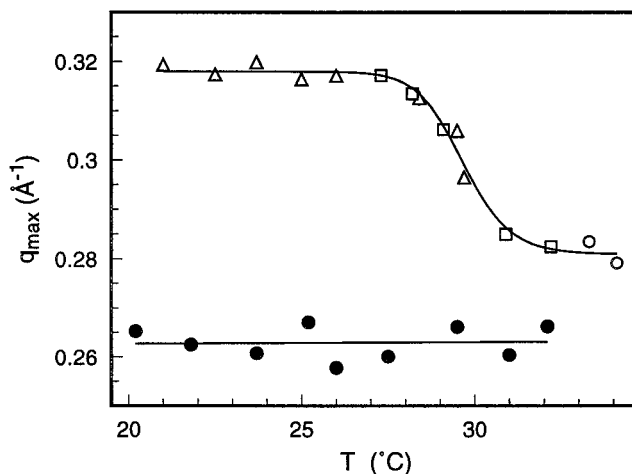

FIGURE 4 The peak position q_{max} of the structure factor $S(q)$ at various temperatures. $S(q)$ was obtained from the scattering intensity $I(q)$ divided by the form factor squared $|F(q)|^2$ (paper I). The peak position of DLPC/gD (●) is independent of temperature within the range shown. DMPC/gD (○, □, △) underwent a phase transition from a gel phase below 27°C to the fluid phase above 31°C. Different open symbols represent different samples. The phase transition was explained in paper I.

coefficient K_a and the thickness compressibility $1/B$: $B = K_a/h_o$ (Evans and Needham, 1987; Needham and Evans, 1988). This gives $B \approx 5.7 \times 10^8$ erg/cm^3. One can also obtain B from the voltage dependence of the bilayer capacitance. Hladky and Gruen (1982) obtained $B \approx 5 \times 10^8$ erg/cm^3 from the measurement by White (1978) on glyceryl monooleate.

2. K_c. K_c of DMPC at 30°C was measured to be 1.1–1.3 × 10^{-12} erg by Fourier analysis of the contours of fluctuating spherical vesicles (Duwe et al., 1990; Meleard et al., 1997) and 0.56 × 10^{-12} erg by the pipette aspiration method (Evans and Rawicz, 1990).

3. $2u_o$ (or D_o). What we measured in paper I was the phosphate-to-phosphate distance (PtP) across the bilayer. This distance includes the hydrocarbon region and the glycerol region (from the phosphate to the hydrocarbons) on both sides of the bilayer. In principle a change in PtP could imply a change in one or both regions. We will now show that, based on the electron density profiles, the thinning of DMPC by gramicidin mostly, if not completely, occurs in the hydrocarbon region. The (unnormalized) scattering density profile ρ_{sc} shown in paper I is linearly related to the true electron density profile ρ by $\rho(z) = c\rho_{sc}(z) + b$, where z is the coordinate along the bilayer normal. The constants b and c can be obtained (see Olah et al., 1991) by fixing the value of ρ at one point and integrating ρ to the total number of electrons in one unit cell of the sample. The normalized DMPC and DMPC/gD (10:1) profiles are shown in Fig. 5 (upper panel). We fixed the center points of both profiles at the value of CH$_3$, 0.17 e/Å^3, somewhat arbitrarily, because of the lack of knowledge of their true values. We then rescale z (by multiplying a constant) of the DMPC profile (shown as the gray curve in Fig. 5, upper panel) so its PtP
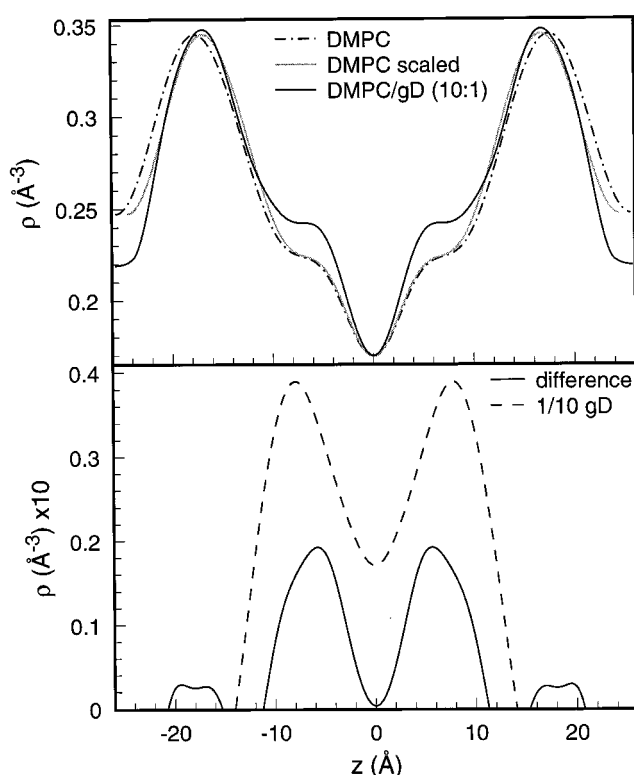
FIGURE 5 Comparison of the electron density profiles of pure DMPC and DMPC/gD in 10:1 ratio. (*Top*) Two profiles are normalized to the total number of electrons in one unit cell, and both of their center points are, somewhat arbitrarily, fixed to the value of CH_3, 0.17 $e/\text{Å}^3$. The z scale of the DMPC profile is adjusted (compressed) to match the peak-to-peak distance of DMPC/gD. (*Bottom*) The solid line shows the difference between the DMPC/gD profile and the rescaled DMPC profile for $|z| < 21$ Å. The dashed line represents the electron density profile of a gramicidin channel (1/10 in amplitude). Note that the length of gramicidin channel is ~26 Å. The difference profile for $|z| > 21$ Å (not shown) reflects the difference in hydration.

matches the PtP of DMPC/gD (10:1). If the thinning (decrease in PtP) by gramicidin occurs in the hydrocarbon region, the rescaled profile of DMPC and the profile of DMPC/gD (10:1) should be different mainly by 1/10 of the electron density profile of gramicidin. To estimate the electron density profile of the gramicidin channel, we took the atomic structure of gramicidin (Woolf and Roux, 1996) and projected the atomic positions on the bilayer normal with a gaussian peak of amplitude Z (the atomic number) and width of 10 Å, normalized by its volume. The result is the dashed line in Fig. 5 (*lower panel*), showing two maxima at $|z| \approx 8$ Å and a minimum at the center. The peaks are caused by the abundance of carbons in the relatively dense backbone and side chains, and the minimum represents the hydrogen bonds between the monomer's terminal groups. The shape of the gramicidin profile reasonably resembles the difference profile. The difference in amplitude could be the artifacts of the normalization procedure (see above). On this basis we assume that the glycerol regions are unchanged between DMPC and DMPC/gD. Using the estimated length of ~5 Å for the glycerol region, we have the

unperturbed hydrocarbon thickness of DMPC $h_o \approx 25.3$ Å and the average thickness in DMPC/gD $\bar{h} \approx 22.7$ Å, compared with the length of the hydrophobic part of the gramicidin channel $h_G \approx 22$ Å (paper I). This gives $2u_o \approx 3.3$ Å and $2\langle u \rangle \approx 2.6$ Å.

4. *s*. The value of *s* will be determined by the requirement that the same value of *s* must produce both the experimental values of $\langle u \rangle$ and the shift in the peak position of $S(q)$ from DLPC/gD to DMPC/gD.

We have modeled the lipid bilayer as a continuous medium that can create a stress field that mediates attraction between gramicidins but otherwise does not hinder the motion of gramicidins. In reality, lipid molecules may adhere to protein molecules. The simulation of free hard disks of diameter 18 Å with the same areal density as gramicidin in DLPC has its first peak of $S(q)$ at 0.3 Å^{-1}, but the peak of $S(q)$ for gramicidin in DLPC is at 0.263 Å^{-1}, corresponding to the most probable nearest-neighbor separation 26.8 Å, which is 8.8 Å larger than the diameter or the contact distance between two hard disks. (Note that the most probable nearest-neighbor separation was obtained by Bessel transform (paper I) and is not equal to $2\pi/q_{max}$ (He et al., 1993a).) We think that this is due to gramicidin's high affinity for the first shell of lipid molecules, making the close encounter between two gramcidins a low-probability occurrence (He et al., 1993a,b). If we were to include this effect, it would certainly increase the number of parameters in simulations and complicate the comparison between the theory and experiment. Thus we will only discuss the mechanism responsible for shifting the peak position of $S(q)$ from 0.263 Å^{-1} in DLPC to 0.283 Å^{-1} in DMPC, an 8% shift. Correspondingly, we seek an ~8% shift in the peak position of $S(q)$ from 0.3 Å^{-1} in the simulation for hard disks free of interactions to 0.324 Å^{-1} in simulations for hard disks in membranes. This peak shift represents the effect of membrane-mediated attraction between the hard disks.

Table 1 lists the simulation parameters corresponding to gramicidin channels (or hard disks) in DMPC. Representative results of the simulations are given in Fig. 6. Fig. 6 *A* shows the simulated position of the first peak in $S(q)$, q_{max}, as a function of *s*. The value of q_{max} for free hard disks is indicated on the graph at 0.304 Å^{-1}. Increasing negative

TABLE 1 Simulation parameters

Simulation	$2u_o$ (Å)	K_c (10^{-12} erg)	B (10^8 erg/cm³)	λ (Å)
1	3.5	0.4	5.0	8.45
2	3.5	1.0	5.0	10.62
3	3.5	2.0	5.0	12.63
4	3.0	0.4	5.0	8.45
5	3.0	1.0	5.0	10.62
6	3.0	2.0	5.0	12.63
7	3.37	0.4	5.0	8.45
8	3.5	0.5	2.5	10.62

DMPC $h_o = 25.3$ Å; channel diameter = 18 Å; number of channels = 81; areal density of channels = 0.29; mesh size = 3.6 Å; $s = -0.1, -0.05, 0, +0.05, +0.1$.
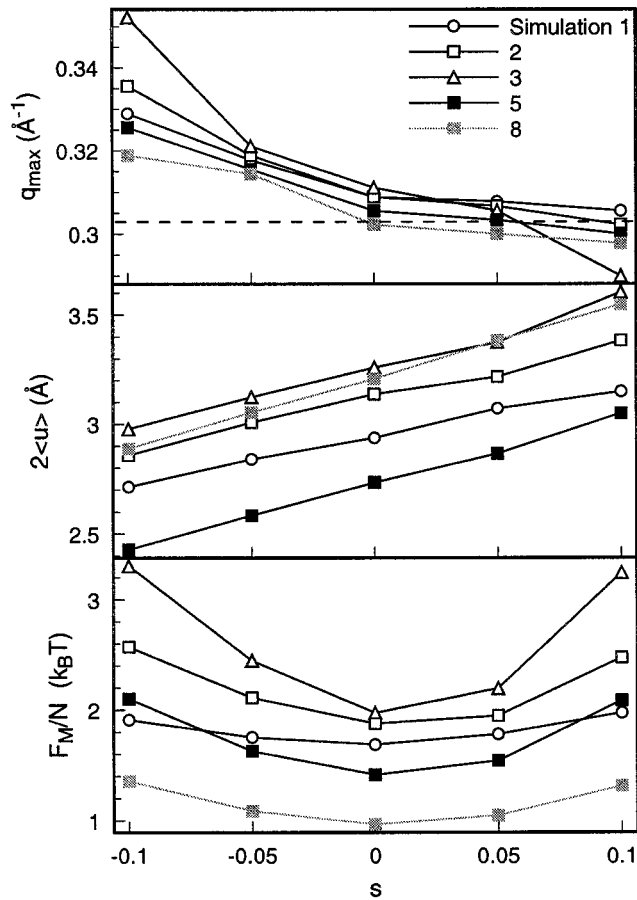
FIGURE 6   Representative results of simulations. The peak position q_{max} of $S(q)$, the average of membrane thinning $2\langle u\rangle$, and the energy of membrane deformation per channel F_M/N are plotted as functions of the boundary slope s. The simulation parameters are listed in Table 1. The dotted line, 0.304 $Å^{-1}$, in the panel q_{max} is the peak position of free hard disks.

produce greater thinning. The main difference between Figs. 6 A and 6 B is in the effect of halving both B and K_c, which has a significant effect on q_{max} but little effect on $\langle u\rangle$. Because $\langle u\rangle$ is determined by the thickness profile that is the solution of Eq. 3, λ is the main determinant for $\langle u\rangle$, not the absolute values of B and K_c. On the other hand, the deformation energy is the determinant for the molecular distributions that determine q_{max}, so q_{max} is sensitive to the absolute values of B and K_c, as well as λ. Note that for all but two cases at $s = 0.1$, the membrane surface is convex, that is, the membrane between channels tends to recover the unperturbed thickness. In the two instances, however, where the boundary gradient has the large positive value of 0.1, the average thinning slightly exceeds the mismatch at the boundaries. This means that the membrane is pinched in the direction of increasing thinning and cannot relax in the spaces between channels.

The energy of membrane deformation per channel as a function of s is shown in Fig. 6 C. Independent of the choice of the parameters, the energy is at minimum at $s = 0$. This contrasts with the case of one channel in an infinite membrane, where the minimum of the deformation energy occurs at a large negative slope, ~ -0.45 (Helfrich and Jakobsson, 1990). However, as discussed earlier, the appropriate value for s at the boundary is not determined by the minimum condition of the deformation energy.

The results of all simulations listed in Table 1 are shown in Fig. 7, where q_{max} is plotted versus $2\langle u\rangle$. The simulations for a chosen set of parameters give a curve in this plot as a function of s. The simulations shown in Fig. 6 are shown here with the same symbols, but their shading is used to indicate different values of s: from the darkest (-0.1) to the lightest ($+0.1$). The experimental results of $2\langle u\rangle$ and the

slope causes the structure factor peak to move to higher values of q, corresponding to smaller separations between channels, hence indicating an increasing attraction between channels. Positive slopes have a lesser and opposite effect (see Fig. 1 for the sign of s). This asymmetry means that the appropriate choice for the sign of the slope will be unambiguous. The desired positive 8% shift in q_{max} can only be achieved with a negative slope. The effect of different values of $\lambda = (h_o K_c/4B)^{1/4}$, the length scale of Eq. 3, which governs the thickness profile, is shown by the results marked by open symbols in Fig. 6 A. Qualitatively, a larger λ means that a deformation will persist further in distance, and therefore there is a greater effect on the mediated interactions. Reducing u_o at the boundary while keeping the same λ diminishes the effect, as expected. Reducing the magnitudes of the elastic constants B and K_c by ½, while keeping the same λ and u_o, also reduces the effect on q_{max}.

The slope has a systematic effect on the average membrane thickness. The average amount of thinning is more or less linear to s, as shown in Fig. 6 B. The effects of varying λ and u_o are similar to those in Fig. 6 A, i.e., larger λ and u_o
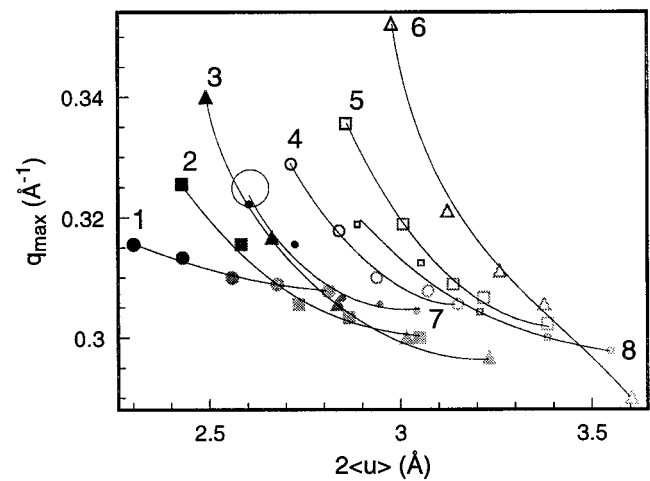

FIGURE 7   The results of all simulations listed in Table 1 plotted as q_{max} versus $2\langle u\rangle$. Each curve (marked by the *simulation number*) is the result of the simulations for a chosen set of parameters (Table 1) as a function of s. The results shown in Fig. 6 are plotted here with the same symbols. Shading is used to indicate different values of s: from the darkest (-0.1) to the lightest ($+0.1$). The experimental results of $2\langle u\rangle$ and the shift in q_{max} are in the circled area.

shift in q_{max} are in the circled area. The three curves with open symbols show that for $2u_o = 3.5$ Å the simulation results approach the target region with decreasing values of λ. With a reduced value of $2u_o$, each group of open symbols becomes its corresponding group of closed symbols. Two curves passing through the target regions are one with $2u_o = 3.0$ Å, $\lambda = 12.63$ Å at $s = -0.07$ and the other with $2u_o = 3.37$ Å, $\lambda = 8.45$ Å at $s = -0.1$. We conclude that, for a reasonable choice of parameters, $2u_o \approx (3.0$ to 3.4 Å), $\lambda \approx (8.5$ to 12.6 Å), $s \approx (-0.10$ to $-0.07)$, the result of gramicidin in DMPC can be explained with the elasticity theory given in Eq. 1.

CONCLUSION

Let us imagine that hydrophobic matching did not occur where a gramicidin channel is inserted and call it the mismatched condition, and compare that with the matching condition schematically shown in Fig. 1 *A*. The relevant energies for comparison are as follows: for the mismatched condition, the mismatch energy E(mis) and the binding energy between the gramicidin surface and first-shell lipids in their unstressed configurations E_{bd1}, and for the matching condition, the deformation energy F_M (per channel) and the binding energy between the gramicidin surface and first-shell lipids in their stressed configurations E_{bd2}. We do not know if E_{bd1} and E_{bd2} are different. We assume that their difference, if any, is small. Thus, for hydrophobic matching to occur, the energy cost of membrane deformation F_M must be smaller than the energy cost of hydrophobic mismatch E(mis). For the example we studied here, gramicidin channels in a DMPC bilayer, E(mis) is $\sim 9.4 \times 10^{-14}\ D_o$ erg $\approx 3.1 \times 10^{-13}$ erg $\approx 7.6 k_B T$ per channel, whereas F_M per channel is $\lesssim 3 k_B T$ (Fig. 6 *C*). We estimated that the upper limit of D_o for a complete hydrophobic matching to occur is ~ 5 Å. However, even if $D_o > 5$ Å, a partial hydrophobic matching may still occur. We also note that these numerical values could be revised by new and better experimental measurements, particularly the energy of mismatch (Chothia, 1974).

Not knowing the boundary condition for the slope s diminishes the predictive power of the theory. For example, suppose that we had only the data on average thinning $\langle u \rangle$. Then, with a free choice of s, one would be able to fit the experimental value of $\langle u \rangle$ with a wide range of values for the elastic constants B and K_c. However, to satisfy both the experimental data on $\langle u \rangle$ and q_{max}, s is restricted to a narrow range of $(-0.10$ to $-0.07)$, even allowing a fairly wide range of values for u_o and λ around their respective estimated values. In the case of one channel in an infinite membrane, we found that s is slightly positive (~ 0.1 for $2u_o \approx 3.5$ Å) to explain the membrane thickness effect on gramicidin channel lifetime (Huang, 1986). Taken together, we suggest that for gramicidin experiments one may use $s = 0$ as first-order approximations (see also Nielsen et al., 1998).

Hydrophobic matching and membrane-mediated interactions are intuitively appealing, and each has been an accepted concept for a long time. As far as we know, they have never been quantitatively analyzed, perhaps owing to a lack of appropriate experimental data. Gramicidin is an ideal protein for testing these idea. Our quantitative analysis shows that the experimental data can be understood in terms of a simple elasticity theory of membrane deformation.

APPENDIX: FINITE DIFFERENCE APPROXIMATION

We used a finite difference approximation method to solve Eq. 3. We laid a square mesh on top of the simulation area, such that $u(x, y)$ becomes $u(i \cdot d, j \cdot d)$, where d is the mesh spacing and i, j are integers. The finite difference approximations of the biharmonic operator in Eq. 3 and the Laplacian in Eq. 2 were all of order d^4 (Abramowitz and Stegun, 1974). The efficiency of the numerical calculation is determined by the method used to solve the resulting matrix equation $\mathbf{Au} = \mathbf{b}$ for vector $\mathbf{u}$, given matrix $\mathbf{A}$ and vector $\mathbf{b}$. The size of $\mathbf{A}$ is $N^2 \times N^2$, where N is the number of mesh points along one edge of the simulation area. In our case, $N = 73$. The preconditioned biconjugate gradient stabilized method of solving matrix equations was coded in the C programming language from the pseudo-code in Barrett et al. (1994), with additional supporting code supplied by Press et al. (1995). The stopping criteria for the iterative solution were set such that the residue $|\mathbf{Au} - \mathbf{b}|$ was less than $10^{-5}|\mathbf{b}|$. The tridiagonal part of $\mathbf{A}$ was used as the preconditioning matrix.

Boundary conditions were applied to those mesh points on and next to every channel. Mesh points on a channel were fixed to the value $\mathbf{u}_o$. Mesh points next to a channel were set to a value that depends on $\mathbf{u}_o$, s, and the distance $r - r_o$ ($\leq d$) from the edge of the channel. If the mesh is chosen finely enough, a linear gradient for the mesh points near a channel would be sufficient, but a fine mesh requires a long computation time. For a coarse mesh, a linear gradient is a poor approximation. Instead we solve Eq. 3 near a channel by assuming the cylindrical symmetry and making a variable change $r = r_o + \rho d$, so that Eq. 3 becomes

$$u'''' + \frac{2d}{r_o} u''' - \frac{d^2}{r_o^2} u'' + \frac{d^3}{r_o^3} u' + \frac{d^4}{r_o^4} u = 0 \qquad (1)$$

where $u' = \partial u / \partial \rho$, etc. A general solution is

$$u(\rho) = C_1 e^{\alpha_1 \rho} + C_2 e^{\alpha_2 \rho} + C_3 e^{\alpha_3 \rho} + C_4 e^{\alpha_4 \rho} \qquad (2)$$

In general, the α_i's are complex; two have positive real parts and two have negative real parts. We ignore the two solutions with positive exponential growth and keep only two solutions in A2 with $\text{Re}[\alpha_i] \leq 0$, say α_1 and α_2. The two coefficients C_1 and C_2 are solved by demanding $\mathbf{u}(\rho = 0) = \mathbf{u}_o$ and $\mathbf{u}'(\rho = 0) = sd$. We then imposed the value

$$u(r - r_o \leq d) = C_1 e^{\alpha_1 (r - r_o)/d} + C_2 e^{\alpha_2 (r - r_o)/d} \qquad (3)$$

on the mesh points next to the channels. This is a good approximation, particularly for negative slope s, except when two channels are so close that there is only one mesh point between them. In that case we take the average of two values, each calculated from the boundary condition of one of the two channels.

REFERENCES

Abramowitz, M., and I. A. Stegun. 1974. Handbook of Mathematical Functions. Dover Publications, New York. 885.

Allen, M. P., and D. J. Tildesley. 1987. Computer Simulations of Liquids. Oxford University Press, New York. 118–123.

Aranda-Espinoza, H. A. Berman, N. Dan, P. Pincus, and S. A. Safran. 1996. Interaction between inclusions embedded in membranes. *Biophys. J.* 71:648–656.

Arseniev, A. S., V. F. Bystrov, T. V. Ivanov, and Y. A. Ovchinnikov. 1985. ^{1}H-NMR study of gramicidin-A transmembrane ion channel. Head-to-head right-handed single-stranded helices. *FEBS Lett.* 186: 168–174.

Barrett, R., M. Berry, T. F. Chan, J. Demmel, J. M. Donato, J. Dongarra, V. Eijkhout, R. Pozo, C. Romine, and H. Van der Vorst. 1994. Templates for the Solution of Linear Systems: Building Blocks for Iterative Methods. SIAM, Philadelphia. 44–45, 56, 74–80.

Boon, J. P., and S. Yip. 1980. Molecular Hydrodynamics. Dover Publications, New York. 279–392.

Chothia, C. 1974. Hydrophobic bonding and accessible surface area in proteins. *Nature.* 248:338–339.

Dan, N., A. Berman, P. Pincus, and S. A. Safran. 1994. Membrane-induced interactions between inclusions. *J. Phys. II France.* 4:1713–1725.

Dan, N., P. Pincus, and S. A. Safran. 1993. Membrane-induced interactions between inclusions. *Langmuir.* 9:2768–2771.

de Gennes, P. G. 1969. Conjectures sur l'etat smectique. *J. Phys. (Paris).* 30 (Colloq. 4, Suppl., 11–12):65–71.

Duwe, H. P., J. Kaes, and E. Sackmann. 1990. Bending elastic moduli of lipid bilayers: modulation by solutes. *J. Phys. France.* 51:945–962.

Elliott, J. R., D. Needham, J. P. Dilger, and D. A. Hayden. 1983. The effects of bilayer thickness and tension on gramicidin single-channel lifetime. *Biochim. Biophys. Acta.* 735:95–103.

Evans, E. A., and D. Needham. 1987. Physical properties of surfactant bilayer membranes: thermal transitions, elasticity, rigidity, cohesion, and colloidal interactions. *J. Phys. Chem.* 91:4219–4228.

Evans, E. A., and W. Rawicz. 1990. Entropy-driven tension and bending elasticity in condensed-fluid membranes. *Phys. Rev. Lett.* 64: 2094–2097.

Fattal, D. R., and A. Ben-Shaul. 1993. A molecular model for lipid-protein interaction in membranes: a role of hydrophobic mismatch. *Biophys. J.* 65:1795–1809.

Goulian, M. 1996. Inclusions in membranes. *Curr. Opin. Colloid Interface Sci.* 1:358–361.

Goulian, M., R. Bruinsma, and P. Pincus. 1993. Long-range forces in heterogeneous fluid membranes. *Europhys. Lett.* 22:145–150.

Goulian, M., O. N. Mesquita, D. K. Fygenson, E. Moses, C. Nielsen, O. S. Andersen, and A. Libchaber. 1998. Gramicidin channel kinetics under tension. *Biophys. J.* 74:328–337.

Hansen, J. P., and K. R. McDonald. 1986. Distribution function theories. *In* Theory of Simple Liquids, 2nd Ed. Academic, New York. 118–119.

Harroun, T. A., W. T. Heller, T. M. Weiss, L. Yang, and H. W. Huang. 1999. Experimental evidence for hydrophobic matching and membrane-mediated interactions in lipid bilayers containing gramicidin. *Biophys. J.* 76:937–945.

He, K., S. J. Ludtke, D. L. Worcester, and H. W. Huang. 1996. Neutron scattering in the plane of membrane: structure of alamethicin pores. *Biophys. J.* 70:2659–2666.

He, K., S. J. Ludtke, Y. Wu, and H. W. Huang. 1993a. X-ray scattering with momentum transfer in the plane of membrane: application to gramicidin organization. *Biophys. J.* 64:157–162.

He, K., S. J. Ludtke, Y. Wu, and H. W. Huang. 1993b. X-ray scattering in the plane of membrane. *J. Phys. France IV.* 3:265–270.

Helfrich, W. 1973. Elastic properties of lipid bilayers: theory and possible experiments. *Z. Natureforsch.* 28C:693–703.

Helfrich, P., and E. Jakobsson. 1990. Calculation of deformation energies and conformations in lipid membranes containing gramicidin channels. *Biophys. J.* 57:1075–1084.

Hladky, S. B., and D. W. R. Gruen. 1982. Thickness fluctuations in black lipid membranes. *Biophys. J.* 38:251–258.

Huang, H. W. 1986. Deformation free energy of bilayer membrane and its effect on gramicidin channel lifetime. *Biophys. J.* 50:1061–1070.

Huang, H. W. 1995. Elasticity of lipid bilayer interacting with amphiphilic helical peptides. *J. Phys. II France.* 5:1427–1431.

Israelachvili, J. 1992. Intermolecular and Surface Forces. Academic Press, New York. 128–135.

Ketchem, R. R., W. Hu, and T. A. Cross. 1993. High-resolution conformation of gramicidin A in a lipid bilayer by solid-state NMR. *Science.* 261:1457–1460.

Lado, F. 1968. Equation of state of the hard-disk fluid from approximate integral equation. *J. Chem. Phys.* 49:3092–3096.

Landau, L. D., and E. M. Lifshitz. 1969. Statistical Physics. Addison-Wesley, Reading, MA. 424–433.

Lang, D. A. 1988. Three-dimensional structure at 86 Å of the uncomplexed form of the transmembrane ion channel peptide gramicidin A. *Science.* 241:188–191.

Marcelja, S. 1976. Lipid-mediated protein interaction in membranes. *Biochim. Biophys. Acta.* 455:1–7.

Meleard, P., C. Gerbeaud, T. Pott, L. Fernandez-Puente, I. Bivas, M. D. Mitov, J. Dufourq, and P. Bothorel. 1997. Bending elasticities of model membranes: influences of temperature and sterol content. *Biophys. J.* 72:2616–2629.

Mouritsen, O. G., and M. Bloom. 1993. Models of lipid-protein interactions in membranes. *Annu. Rev. Biophys. Biomol. Struct.* 22:145–171.

Needham, D., and E. Evans. 1988. Structure and mechanical properties of giant lipid (DMPC) vesicle bilayers from 20C below to 10C above the liquid crystal-crystalline phase transition at 24C. *Biochemistry.* 27: 8261–8269.

Nicholson, L. K., and T. A. Cross. 1989. Gramicidin cation channel: an experimental determination of the right-handed helix sense and verification of β-type hydrogen bonding. *Biochemistry.* 28:9379–9385.

Nielsen, C., M. Goulian, and O. S. Andersen. 1998. Energetics of inclusion-induced bilayer deformations. *Biophys. J.* 74:1966–1983.

Olah, G. A., H. W. Huang, W. Liu, and Y. Wu. 1991. Location of ion binding sites in the gramicidin channel by x-ray diffraction. *J. Mol. Biol.* 218:847–858.

Owicki, J. C., and H. M. McConnell. 1979. Theory of protein-lipid and protein-protein interactions in bilayer membranes. *Proc. Natl. Acad. Sci. USA.* 76:4750–4754.

Pearson, L. T., J. Edelman, and S. I. Chan. 1984. Statistical mechanics of lipid membranes. Protein correlation functions and lipid ordering. *Biophys. J.* 45:863–871.

Press, W. H., S. A. Teukolsky, W. T. Vetterling, and B. P. Flannery. 1995. Numerical Recipes in C, 2nd Ed. Cambridge University Press, Cambridge. 78–89, 331, 373–374.

Schroeder, H. 1977. Aggregation of proteins in membranes: an example of fluctuation-induced interactions in liquid crystals. *J. Chem. Phys.* 67: 1617–1619.

Seddon, J. M. 1989. Structure of the inverted hexagonal (H_{II}) phase, and non-lamellar phase transitions of lipids. *Biochim. Biophys. Acta.* 1031: 1–69.

Tanford, C. 1980. The Hydrophobic Effect: Formation of Micelles and Biological Membranes. Wiley, New York. 1–4.

Wallace, B. A., and K. Ravikumar. 1988. The gramicidin pore: crystal structure of a cesium complex. *Science.* 241:182–187.

White, S. H. 1978. Formation of solvent-free black lipid bilayer membranes from glyceryl monooleate dispersed in squalene. *Biophys. J.* 23:337–347.

Woolf, T. B., and B. Roux. 1996. Structure, energetics, and dynamics of lipid-protein interactions: a molecular dynamics study of the gramicidin A channel in a DMPC bilayer. *Proteins.* 24:92–114.